Tightening of the elastic overhand knot

Sylwester Przybyl and Piotr Pieranski*
Poznan University of Technology, Nieszawska 13A, 60-965 Poznan, Poland
(Received 20 February 2008; published 12 March 2009)

The process of tightening of the open trefoil knot tied on an elastic filament is analyzed. Evolution of the curvature profile is presented and discussed.

DOI: 10.1103/PhysRevE.79.031801 PACS number(s): 36.20.−r, 46.25.−y, 46.70.Hg

I. INTRODUCTION

Most of knots used in the everyday life are open [1]. As a rule, the knots become useful when they are brought to tight conformations since only then friction prevents them from untying. The most tight conformations of a few simple knots have been studied previously. In Ref. [2], Saitta *et al.* presented results of a numerical simulation in which the overhand knot tied on an *n*-decane molecule was subject to the tightening. The authors reported appearance of sharp curvature maxima located close to the entrances of the knot. In Ref. [3] we analyzed in detail the curvature and torsion profiles of the 3_1 (overhand) and 4_1 (figure eight) open knots tied on the slippery floppy hard rope, i.e., such a model of the real rope in which one assumes that it is perfectly slippery and floppy but at the same time perfectly hard in its circular sections. The study also indicated that curvature of the tightest conformations of the knots tied on such a rope reaches its maximum close to the entrance where characteristic asymmetric double peaks are observed. Following the observation a hypothesis was formulated that real ropes, on which the knots were tied, would break at the maximum curvature points. Experiments performed with knots tied on cooked spaghetti [4] verified positively the hypothesis while analogous experiments carried out with a poly(vinylidene fluoride) fishing line contradicted it by demonstrating that overhand knots tied on such filament brake at a points located inside the knots, far from the entrance [5].

Recently, Audoly *et al.* [6] presented an approximate theoretical analysis of laboratory experiments in which single and multiple overhand knots were tied and tightened on an elastic rod of nitinol. The authors demonstrated convincingly that their approximate theory describes well a number of experimentally established facts such as the appearance of very thin gaps in the braided regions of the tightened knots. Encouraged by the success of their theory in the description of knots at the beginning of their tightening process the authors presented in Sec. IV some preliminary results concerning the final stages of the process and confronted them with results of our numerical study of the most tight overhand knot tightened on a floppy rope [3]. In Fig. 6 they plotted the theoretically predicted curvature profile of the overhand knot in a more tight state indicating the cusplike maxima localized close to the center of the knot. Subsequently they formulated a conjecture that the much higher and differently localized maxima we described for knots tied on floppy ropes do not appear in knots tied on elastic rods since they are "regularized by elasticity." It is our aim to falsify this conjecture by presenting results of a precise numerical study of the evolution of the curvature profile for the overhand knot tightened on the slippery elastic hard rope (SEHR). We shall demonstrate that although in the initial stage of the tightening process the maximum curvature points are indeed localized inside the knot, at the end of it, four new, distinct maxima appear close to the entrance of the knot.

II. NUMERICAL PROCEDURES

Before the results of numerical simulations that we have performed are discussed, let us present the hypothetical laboratory experiment that the simulations are aimed to mimic. A piece of SEHR of length L and radius $R=1$, on which the overhand knot has been tied, is stretched between two points located at a distance $d<L$. The whole knot should be seen as submerged in a high viscosity fluid which overdamps its dynamics (see Fig. 1). Subsequently, the distance d is enlarged in steps until the knot becomes perfectly tight. At each step of the tightening process, the knot finds spontaneously free from overlap conformation that minimizes its elastic energy [7],

$$U_E = \frac{1}{2}E\int_0^L \kappa^2(s)ds, \tag{1}$$

where $\kappa(s)$ is the curvature profile of the knot, i.e., the dependence of its curvature κ on the arc-length parameter s and E is the elastic (bending) modulus of the rope. What happens in nature spontaneously must be simulated in numerical calculations by an appropriate algorithm. For the sake of brevity, we do not present here all its technical details. Let us present, however, its basic assumptions.

The numerical model of the rope, on which the studied overhand knot has been tied, is discrete. The rope is represented in the simulations by a sequence of equidistant N points $\mathbf{v}_i=(x_i,y_i,z_i)$, $i=1,2,\ldots,N$ referred to in what follows as vertices; thus, the simulated knot consists of $N-1$ stiff

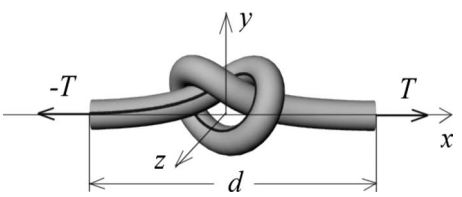

FIG. 1. Geometry of the simulated tightening experiment.

*piotr.pieranski@put.poznan.pl

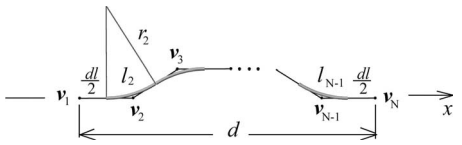

FIG. 2. Details of the inscribed knot construction.

segments $\mathbf{e}_i=\mathbf{v}_i-\mathbf{v}_{i-1}$, $i=2,3,\ldots,N$ of a fixed common length dl. From the practical point of view the simulated knot is thus equilateral. Let us denote it by K_p.

As indicated by Rawdon [8], it is possible to inscribe into K_p a continuous knot K_c of piecewise constant curvature. Its elastic energy is given by the sum,

$$U_E = \frac{1}{2}E\sum_{i=2}^{N-1}\frac{l_i}{r_i^2}, \tag{2}$$

where r_i is the curvature radius of the arc inscribed into the ith corner of the polygonal knot and l_i is the length of the arc. To make the definition of the inscribed knot complete, we treat the first half of the first segment and the second half of the last segments as shorter arcs of zero curvature. Thus, $l_1=l_N=\frac{dl}{2}$ and $r_1=r_N=\infty$.

The based on the finite element method (FEM) algorithm developed by one of us (S.P.) aims at minimizing the elastic energy of the knot by changing orientations of its segments but guarding it at the same time from self-overlapping. From the physical point of view the algorithm simulates the hypothetical laboratory experiment described at the beginning of the present section.

During the simulations the end vertices of the knot, $\mathbf{v}_1$ and $\mathbf{v}_N$, are fixed on the x axis of the reference frame, however, the spatial orientations of the first and the last segments remain free. From the physical point of view such boundary conditions imply that the end vertices of the knot are subject to tension T, but no torque is applied to the end segments.

The distance between the ends of the tightened knot

$$d = x_N - x_1, \tag{3}$$

while the length of the inscribed knot K_c

$$L_c = \frac{dl}{2} + \sum_{i=2}^{N-1} l_i + \frac{dl}{2} \tag{4}$$

(see Fig. 2). The simulation itself and the postsimulation calculations are carried out in such a manner that eventually the subject to analysis that inscribed knot may be seen as free from self-overlap knot tied on a SEHR of unit radius: $R=1$.

All details of the inscribed knot construction and its further interpretation are described in detail in Ref. [8], where we applied the method of Rawdon [8] for interpretation of the closed trefoil knot tied and tightened on SEHR by the shrink or no overlaps (SONO) algorithm. The FEM algorithm that we have used here is different, but since the structure of the subject to the algorithm polygonal knot is the same, the technique of Rawdon [8] applies without any changes.

At the end of each of the FEM runs carried out at different values of d, the coordinates of the vertices of the final conformation were registered. Using the data we subsequently calculated the effective knot length of the inscribed knot $L_K=L_c-d$, its the curvature profile $\kappa(s)$, and its total elastic energy U_E defined by Eq. (2). As mentioned above, due to the particular construction of the inscribed knot K_c its curvature profile is piecewise constant. To formulate its formal description let us introduce first the sequence of the discrete values of the arc-length parameter s,

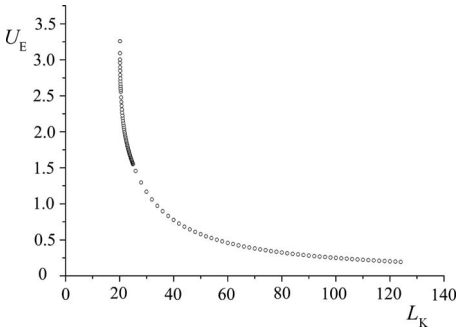

FIG. 3. Energy of the overhand knot tightened on a slippery, hard, elastic rope of radius $R=1$ vs the effective knot length L_K ($E=1$).

$$s_0 = -\Delta,$$

$$s_1 = s_0 + \frac{dl}{2},$$

$$s_i = s_{i-1} + l_i, \quad i = 2,3,\ldots,N-1,$$

$$s_N = s_{N-1} + \frac{dl}{2} = L_c - \Delta. \tag{5}$$

$\Delta \approx \frac{L_c}{2}$ is an experimentally determined value shifting the arc-length parameter s so that the center of symmetry of the simulated knot would be located at $s=0$. This simplifies visual analysis of all plots.

Assuming that r_1 and r_N are infinite and using the defined above s_i values one may define the piecewise constant curvature profile of the inscribed knot as

$$\kappa(s) = \frac{1}{r_i}, \quad s \in (s_{i-1}, s_i), \quad i = 1,3,\ldots,N. \tag{6}$$

For the sake of an easier analysis of the presented below results in terms in Ref. [6], we shall also use there the defined variable,

$$\epsilon = \sqrt{\frac{2\pi}{L_K}}. \tag{7}$$

III. RESULTS

The most essential characteristic of a knot tied on SEHR is the dependence of its elastic energy U_E on the effective knot length L_K. Figure 3 presents the plot of the whole dependence obtained from our simulations. Precise values of

TABLE I. Energy of the overhand knot tightened on a slippery, hard, elastic rope of radius $R=1$ vs the effective knot length L_K ($E=1$).

L_K	ϵ	U_E
120.06	0.2288	0.200
84.041	0.2734	0.305
66.032	0.3085	0.407
48.023	0.3617	0.609
40.019	0.3962	0.775
32.015	0.4430	1.061
28.013	0.4736	1.295
25.003	0.5013	1.550
23.603	0.5160	1.711
23.203	0.5204	1.765
22.302	0.5308	1.911
21.502	0.5406	2.094
20.902	0.5483	2.309
20.501	0.5536	2.553
20.381	0.5552	2.666
20.196	0.5578	3.258

the energy are here crucial since, if the results of our simulations were to be compared with results obtained by other authors, one should first compare values of the elastic energy. To make such a comparison easier we provide also a table within which some of the values plotted in Fig. 3 are given (see Table I).

Since the elastic energy U_E of a knot tightened on SEHR is directly connected with its curvature profile $\kappa(s)$, we present also evolution of the latter versus the effective knot length L_K (see Fig. 4). The figure covers the range of L_K from 25.00 to 20.20 which in terms of the ϵ parameter is equivalent to the interval (0.50, 0.56).

Before we look at the shapes of a considerably tightened overhand knot let us first analyze it in the case of a loose knot $L_K=80$. Figure 5 presents the details of its structure. We clearly see two isolated points of self-contact and a short braided region. In the intervals between the braided region

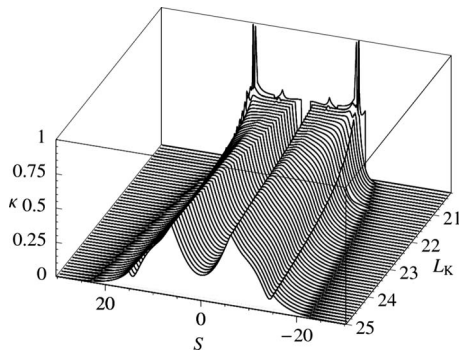

FIG. 4. Evolution of the curvature profile of the overhand knot tied and tightened on the slippery, hard, elastic rope vs the effective knot length L_K. In terms of the ϵ parameter the plot covers its range from 0.50 to 0.56.

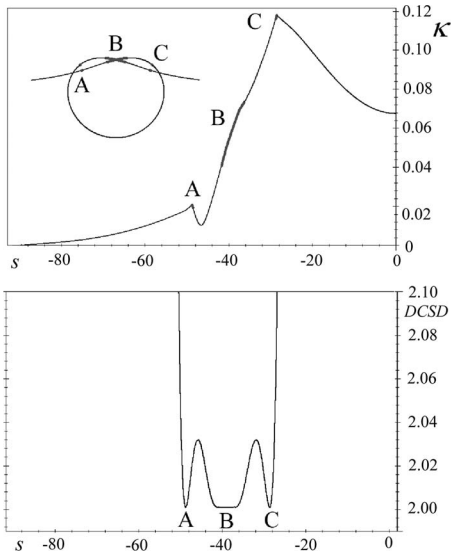

FIG. 5. Details of the shape of a loose overhand knot: $L_K=80.00$ ($\epsilon=0.28$). A half of the curvature profile is shown in the upper part of the figure. With the thick line we marked the places, in which the knot remains in a self-contact as indicated by the lower part of the figure, where the doubly critical self-distance is plotted.

and the isolated contact points one observes the very thin gaps described in Ref. [6]. As the knot becomes tightened, the braided region becomes wider which limits the space left for the gaps. Figure 6 presents the curvature profiles found at $L_K=25.00$ ($\epsilon=0.50$) and $L_K=23.20$ ($\epsilon=0.52$).

Looking at the curvature profile at $L_K=23.20$ ($\epsilon=0.52$) we clearly see that the gaps have vanished—the isolated points of contacts joined the growing braided region. Comparing the curvature profile with the profile presented by authors in Ref. [6], in Fig. 6 we see a clear qualitative difference: the central cusplike maxima reported in Ref. [6] are not present in our curvature profile.

The gaps reported in Ref. [6] vanish at $L_K=24.50$. Close to the same value of L_K maxima marked as C in the curvature profile reaches $\frac{1}{2}$ value, which is characteristic to the situation when one piece of the rope winds tightly around another piece of it. This ends the first stage of the knot tightening process.

In the second stage of the tightening, covering the effective knot lengths from 24.50 to 20.55, the curvature profile

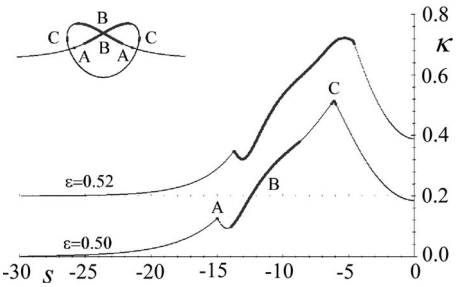

FIG. 6. Details of the curvature profiles found at $L_K=25.00$ ($\epsilon=0.50$) and $L_K=23.20$ ($\epsilon=0.52$). The latter profile has been shifted up by 0.2. Regions at which the knot remains in the self-contact are marked with thick lines. Since the profiles are symmetrical we presented only a representative half of them.

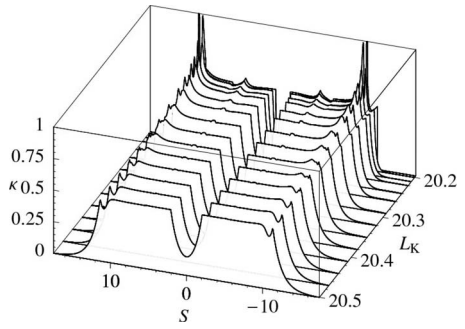

FIG. 7. Evolution of the curvature profile at the end of the tightening process. $L_K \in (20.50, 20.20)$.

develops almost flat parts located around $\kappa=0.5$. At the same time the outer maxima localized at the entrances of the knot shift up. As a result, at the end of this stage, except for the middle part of the knot, where the rope remains free from self-contacts, the curvature profile is almost flat.

The third end stage of the tightening process is shortest but most subtle. It covers the range of L_K from 20.50 to 20.20. One observes here formation of double peaks of curvature located at the entrance of the knot (see Fig. 7). These are the maxima, which we have reported in [3] and whose existence in knots tied on an elastic rope has been put in doubt by Audoly *et al.* in Ref. [6]. Figure 7 provides the direct proof that the maxima are not regularized by elasticity.

Let us analyze the dependence of the knot energy U_E on its decreasing effective length L_K. Although the changes in the effective knot length are here very small, its energy grows very rapidly (see Fig. 8). Let us emphasize that although the rate at which energy grows becomes infinite as the knot approaches its most tight conformation, the final value of energy is finite. As we have found out the growth of energy is well described by the formula having the following form:

$$U_E = U_E^{\max}(1 - \alpha\delta^{\gamma}), \tag{8}$$

where

$$\delta = \frac{L_K - L_K^{\min}}{L_K^{\min}}. \tag{9}$$

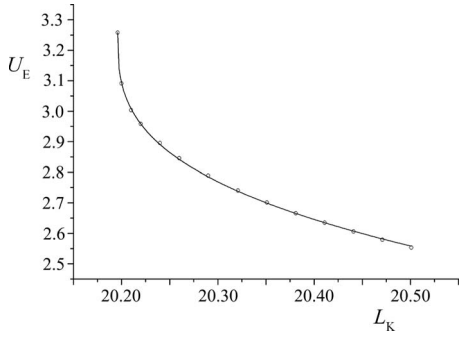

FIG. 8. Dependence of the elastic energy U_E on effective knot length L_K observed for the overhand knot tied on SEHR at the end of the tightening process.

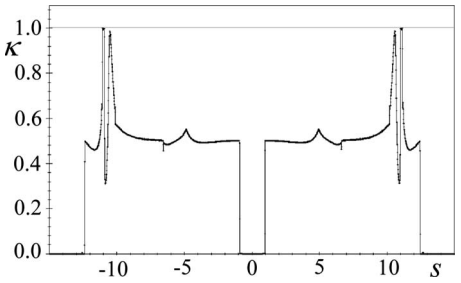

FIG. 9. Curvature profile of the most tight overhand knot tied on the slippery elastic hard rope.

Numerical analysis provides the following values of the parameters: $\alpha=0.869$ and $\gamma=0.333$. The final value of energy $U_E^{\max}=3.258$ and it is located at $L_K^{\min}=20.196$. This is the length at which the knot subject to the infinite tension T reaches its most tight conformation $K^{\min}$. Figure 9 presents its curvature profile. The double peaks noticed in Ref. [3] located close to the entrance are well visible. Higher accuracy of the present simulations allows us to get a better insight into the tightest knot structure. The most essential observation is that the curvature hits the upper limit $\kappa=1$ imposed by the condition that the rope is hard in its circular sections. Let us also notice that as expected in this most tight conformation the ends and the middle parts of the knot are straight, i.e., their curvature is equal to zero.

IV. CONCLUSIONS

Numerical simulations whose results we presented above demonstrated clearly that maxima of curvature of the overhand knot tied on an elastic rope change their positions during the tightening process. For small tensions applied to the free ends of the knot the maxima are located inside the knot but as the tension becomes high, the maxima turn into almost flat plateau and eventually, at the end of the tightening process, much higher double peaks of curvature appear close to the entrance of the knot. The theory developed by Audoly *et al.* [6] is not able to account for this phenomenon. This result is essential in the discussion on the position of the breaking point since it indicates that whether the knot subject to tension will break at a point located close to its center or close to its entrance depends on the stage of the tightening process at which the breaking happens. Let us, however, point out that, as indicated by the experimental study performed by Uehara *et al.* [5], the problem of the knot breaking is more complex and considering it within the hard rope models may be not sufficient. It seems necessary to take into account not only the curvature profile of the knotted rope but also the profile of the deformation of its perpendicular sections. This needs working with such models of the rope that are not hard.

ACKNOWLEDGMENT

This work was supported by Poznan University of Technology under Grant No. PB-DS 62-176.

[1] C. W. Ashley, *The Ashley Book of Knots* (Doubleday, New York, 1993).
[2] A. M. Saitta, P. D. Soper, E. Wasserman, and M. L. Klein, Nature (London) **399**, 46 (1999).
[3] P. Pieranski, S. Przybyl, and A. Stasiak, Eur. Phys. J. E **6**, 123 (2001).
[4] P. Pieranski, S. Kasas, G. Dietler, J. Dubochet, and A. Stasiak, New J. Phys. **3**, 10 (2001).
[5] H. Uehara, H. Kimura, A. Aoyama, T. Yamanobe, and T. Komoto, New J. Phys. **9**, 65 (2007).
[6] B. Audoly, N. Clauvelin, and S. Neukirch, Phys. Rev. Lett. **99**, 164301 (2007).
[7] R. Gallotti and O. Pierre-Louis, Phys. Rev. E **75**, 031801 (2007).
[8] J. Baranska, P. Pieranski, S. Przybyl, and E. J. Rawdon, Phys. Rev. E **70**, 051810 (2004).